

Meso scaling of Reynolds shear stress in turbulent channel and pipe flows

T. Wei¹, P. McMurtry¹, J. Klewicki¹, and P. Fife²

¹*Department of Mechanical Engineering*

²*Department of Mathematics*
University of Utah

Salt Lake City, Utah 84112

(Dated: September 15, 2004)

This paper presents experimental and numerical data of the Reynolds shear stress in turbulent channel and pipe flows under a meso-normalization. The meso-length scale associated with this normalization is intermediate to the traditional inner and outer lengths. Justification for the meso-scales is provided by a direct analysis of the mean momentum equation. Specifically, the meso-normalization is revealed through a rescaling that appropriately reflects the physics of an internal meso-layer within which a balance breaking and subsequent balance exchange of terms in the mean momentum equation takes place. The maximum Reynolds shear stress locations and values are also presented. Examination of data reveals that the Reynolds shear stress has different scaling at low Reynolds numbers, while at high Reynolds numbers the data agree well with the new scaling, supporting the new theory.

PACS numbers:

I. INTRODUCTION

Turbulent duct flows are commonplace. A distinguishing characteristic of these (and all turbulent) flows is that the rate of momentum transport is elevated relative to their laminar counterparts. Because of this characteristic, turbulent duct flows are especially important to a large number of technological applications. The origin of this enhanced momentum transport is the intrinsically, but imperfectly, correlated nature of the turbulent fluctuations. This underlying organization of the flow is manifested as an apparent stress gradient owing to the net effect of the inertial terms in the differential statement of Newton's second law – when subjected to the Reynolds decomposition and averaged over time. Of course, the appearance of these Reynolds stress gradients renders the mean balance equation indeterminate. In the case of statistically stationary, fully developed, flow in a pipe or channel, there is only one non-zero stress gradient, $-d\langle uv \rangle / dy$, where u and v are the axial and wall-normal velocity fluctuations respectively, y is the coordinate normal to the wall and angle brackets denote time averaging. For this reason, over the past century a major effort of turbulence research has been associated with the measurement, modeling and Reynolds number scaling of $-\langle uv \rangle$. The present effort focuses on the last of these.

Despite the importance of the Reynolds shear stress relative to momentum transport, its proper scaling remains an open question. Challenges limiting progress relate to the scarcity of high quality data sets that also span a useful Reynolds number range. That is, the difficulties inherent to

measuring the Reynolds shear stress at any fixed Reynolds number are compounded by the requirement to maintain good spatial resolution with increasing Reynolds number (see, for example, DeGraaff and Eaton.¹) In this regard, Direct Numerical Simulations (DNS) provide exceptionally smooth data, but, unfortunately, are limited to relatively low Reynolds numbers. On the other hand, data from physical experiments can be obtained at higher Reynolds numbers, but inherently exhibit greater scatter.

Overall, the vast majority of Reynolds stress data reported in the literature are shown under either inner or outer normalization.² Inner normalization utilizes the friction velocity, $u_\tau = \sqrt{\tau_{wall}/\rho}$ (where τ_{wall} is the mean wall shear stress, and ρ is the mass density), and the kinematic viscosity, ν . Outer normalization utilizes the channel half-height or boundary layer thickness, δ . Existing data reveal that inner normalization results in the different Reynolds number profiles merging to a single curve (i.e., is successful) only out to about 20 viscous units from the wall.¹ This is a much smaller scaling domain than for the inner normalized mean velocity profile – an intriguing point given that the mean velocity and Reynolds shear stress are the two dependent variables in the same mean momentum balance. Outer normalization successfully scales the Reynolds stress profiles over a large portion of the flow in which the distance from the wall is of the same order as the channel half-height (or boundary layer thickness). As is well-known, for channel or pipe flows this normalization is given theoretical support by outer-normalizing the mean momentum balance, neglecting the viscous stress gradient term (owing to

the appearance of a small multiplicative parameter on this term), and integrating once.³ Interestingly, neither inner nor outer normalizations are successful in the vicinity of the peak in the Reynolds stress profile. The present effort explicitly addresses this issue.

The normalization of the Reynolds stress described herein is based on the multiscale analyses of Wei et al.⁴ and Fife et al.⁵ These studies describe a newly revealed layer structure for wall bounded flows that is based upon the properties of the mean momentum balance. Their multiscale analyses are rigorous with regard to turbulent pressure driven pipe and channel flows, as well as turbulent Couette flow. (For the zero pressure gradient boundary layer, the mean momentum equation has been empirically shown to exhibit a highly similar balance breaking and exchange of terms.) Herein, normalizations directly obtained from the multi-scale analysis are shown to render the Reynolds stress profiles invariant with Reynolds number from the lower edge of the meso-layer to the channel half-height. This zone of validity is explicitly shown to be in agreement with the “scaling patch” appropriate for meso-normalization.⁶

II. TRADITIONAL SCALING OF REYNOLDS SHEAR STRESS

A rational starting point for a scale analysis of the Reynolds stress is the properly scaled mean momentum equation. The inner scaled mean momentum equation for fully developed channel or pipe flow is

$$0 = \epsilon^2 + \frac{d^2 U^+}{dy^{+2}} + \frac{dT^+}{dy^+}, \quad (1)$$

where $\epsilon^2 = 1/(\frac{\delta u_\tau}{\nu}) = 1/\delta^+$, U^+ is the inner normalized streamwise velocity, $T^+ = -\langle u^+ v^+ \rangle$ is the inner normalized Reynolds shear stress, δ is the channel half height or pipe radius, and u_τ is the friction velocity. The boundary conditions are $U^+ = T^+ = 0$, $\frac{dU^+}{dy^+} = 1$ at the wall.

Provided ϵ^2 is small, Equation 1 expresses a balance between viscous stress gradients and Reynolds stress gradients. The rationale underlying inner scaling is that in the inner region, the Reynolds number dependence can be neglected in the inner normalized equations (either momentum equation or the integrated momentum equation), as well as in the boundary conditions. This implies similarity (Reynolds number independence) of the inner normalized variables U^+, T^+ as functions of y^+ . This argument is valid at least in a region next to the wall of width $O(1)$ in y^+ .

The outer scaled mean momentum equation for the fully developed channel or pipe flow is

$$0 = 1 + \epsilon^2 \frac{d^2 U^+}{d\eta^2} + \frac{dT^+}{d\eta}, \quad (2)$$

where $\eta = \frac{y}{\delta}$ is the outer normalized distance from the wall. For large Reynolds number the outer normalized mean momentum equation indicates a balance between pressure gradients (or mean advection in flat plate boundary layer) and the Reynolds stress gradient.

The inner normalized Reynolds shear stress profiles for different Reynolds number flows are shown in FIG. 1(a). While the mean streamwise velocity profiles exhibit good agreement with inner scalings for a large range of y^+ (Traditionally it has been claimed that the inner scaled law of the wall describes the mean velocity profile in the viscous sub-layer, buffer layer and log-layer which covers from the wall to $y^+ \leq 0.2\delta^+$ or $\eta < 0.2$, i.e., $y^+ \leq 80$ for $Re_\tau = 395$), the validity of the inner scaling for the Reynolds shear stress profiles is limited to a much smaller region near the wall. Except very close to the wall (say, $y^+ < 10$ to 20), the inner scaling provides a poor characterization of the scaling of the Reynolds shear stress. The inner normalized peak Reynolds shear stress location moves outward with increasing Reynolds number, while the inner normalized maximum Reynolds shear stress value increases and apparently approaches 1 with increasing Reynolds number. This is very clearly shown in FIG. 1(a).

The outer scaling of Reynolds shear stress is based on the outer scaling of the mean momentum equation. For large Reynolds number (small ϵ^2) the outer scaled mean momentum equation is

$$0 = 1 + \frac{dT^+}{d\eta}. \quad (3)$$

Integrating and applying the boundary conditions gives

$$T^+ = 1 - \eta, \quad (4)$$

yielding a Reynolds number independent linear variation with η . This form is valid in the region where, from equation 2, the pressure gradient and Reynolds stress gradient are in nominal balance.

The outer normalized Reynolds shear stress profiles for different Reynolds number flows are shown in FIG. 1(b). The outer scaling merges the data quite well away from the wall (say, $\eta > 0.2$). It is also clear from the data that the outer normalized maximum Reynolds shear stress location moves inward with increasing Reynolds number.

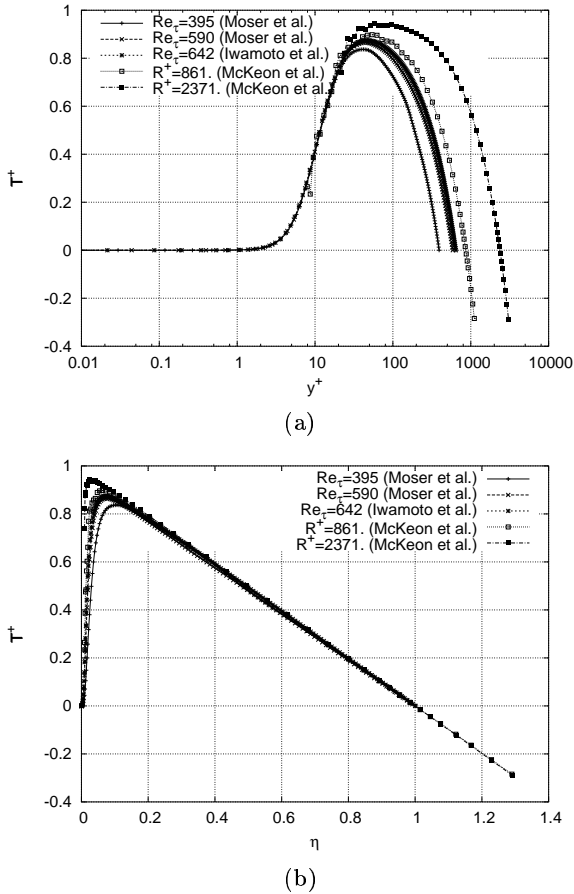


FIG. 1: Traditional scaling of Reynolds shear stress, T^+ . (a). Inner scaling. (b). Outer scaling. (Note that the negative values for $\eta > 1$ of the superpipe flow data are due to the change of the Reynolds shear stress direction across the centerline.)

III. REYNOLDS SHEAR STRESS PEAK VALUE AND LOCATION

The inner scaling and outer scaling of Reynolds shear stress as shown in FIG. 1(a) and FIG. 1(b) illustrate that there is a significant region (in inner normalized wall units), between about $y^+ \sim 20$ and a location beyond the peak in the Reynolds stress that is not properly described by either the inner or outer scaling. The meso-scaling presented in this paper specifically applies in this region around the peak Reynolds shear stress location. In this section the data on the peak Reynolds shear stress location and value are first summarized and compared with results of the multiscale analysis of Wei et al.⁴ and Fife et al.⁵ The value of the maximum Reynolds shear stress and its location have been extracted from DNS data and experimental data for a range

of Reynolds numbers. Relative to the low Reynolds number DNS results, the scatter is greater of experimental data around the maximum Reynolds shear stress location.

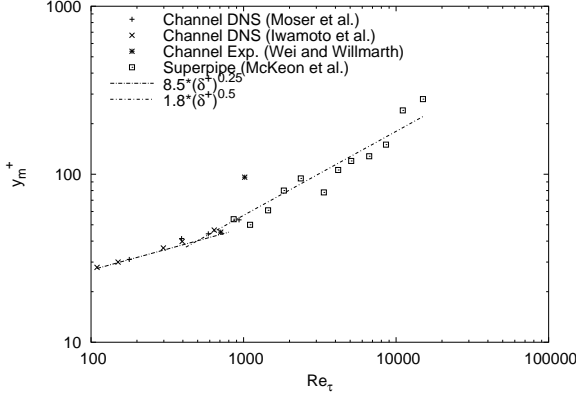
It has been well recognized that the peak Reynolds shear stress location, y_m^+ , is proportional to the square root of Re_τ^{7-10} , i.e., $y_m^+ = C Re_\tau^{0.5}$ (C is roughly between 1.8 and 2.0). This relationship is also supported by the multiscale analysis of Wei et al.⁴ and Fife et al.⁵ Specifically, the multiscale analysis of the mean momentum equation by Wei et al.⁴ yields the following: a) The inner normalized peak location varies with Re_τ as $y_m^+ \sim Re_\tau^{0.5}$, and b) The Reynolds number dependence of the inner normalized maximum Reynolds shear stress, (T_m^+) , was shown to deviate from a possible maximum of 1 (at infinite Reynolds number) as $1 - T_m^+ \sim Re_\tau^{-0.5}$.

The peak Reynolds shear stress location, y_m^+ , data are shown in FIG. 2, as a function of Re_τ or $\frac{1}{\epsilon^2}$. At high Reynolds number the $Re_\tau^{0.5}$ dependence of the peak location is seen. At low Reynolds number the trend line deviates from the theory. This is not unexpected since the theory predictions are arrived at under the assumption of high Reynolds number. For high enough Reynolds number, the data strongly support the theoretical results. FIG. 2(b) is plotted as $y_m^+/\sqrt{Re_\tau}$ versus Re_τ .

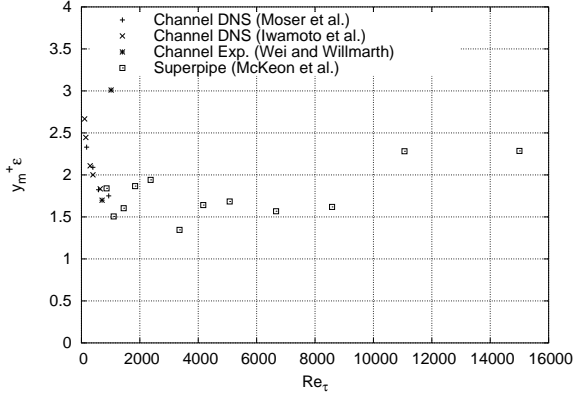
Maximum Reynolds shear stress, T_m^+ , data are presented in FIG. 3 as the deficit from 1, $1 - T_m^+$. At high Reynolds number, the theory and data are in good agreement, but show increasing deviation at low Reynolds number, which again is not unexpected.

IV. MESO SCALING OF THE REYNOLDS SHEAR STRESS

For large Reynolds number (small ϵ), the inner scaled mean momentum equation (Eq. 1) implies a balance between the viscous stress gradient and Reynolds stress gradient, while the outer scaled equation (Eq. 2) implies a balance between the pressure gradient and Reynolds shear stress. Wei et al. have provided an analysis of wall bounded flow based on the relative magnitudes of force balances in the boundary layer and provided a physically based layer structure reflecting these force balances. As pointed out by Wei et al., the transition between inner and outer scaling requires a breaking and exchange of the force balances identified above. In particular, this balance exchange requires a balance among all three terms in the mean momentum equation in an intermediate region (mesolayer) between the inner and outer layers.



(a)



(b)

FIG. 2: Reynolds stress peak location dependence on Reynolds number. (a). y_m^+ versus Re_τ . (b). $\frac{y_m^+}{\sqrt{Re_\tau}}$ versus Re_τ . The DNS data of this paper are from Moser et al.¹¹ Iwamoto et al.¹² The experimental data are from Wei and Willmarth¹³ and McKeon et al.¹⁴

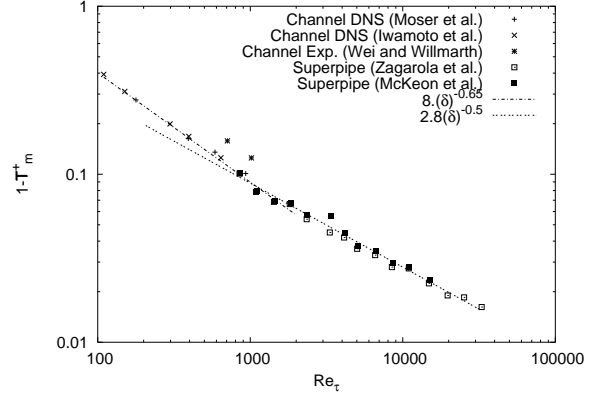
Applying a differential scaling (Fife et al.⁵), a proper meso scaling that formally yields all terms in the mean momentum equation to be of the same order is

$$\hat{y} = \epsilon(y^+ - y_m^+), \quad \hat{T} = \frac{1}{\epsilon}(T^+ - T_m^+). \quad (5)$$

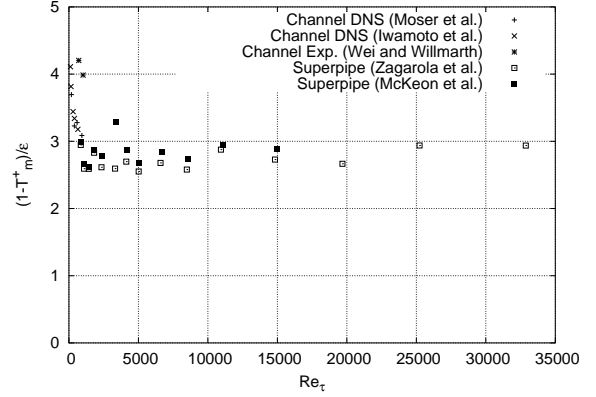
The mean momentum equation under this meso scaling is

$$\frac{d^2 U^+}{d\hat{y}^2} + \frac{d\hat{T}}{d\hat{y}} + 1 = 0. \quad (6)$$

The absence of a small parameter in Equation 6 properly reflects the fact that all the terms are of the same order of magnitude, and thus provides the validity of the \hat{T} and \hat{y} scaling in the mesolayer. Note further that since $d\eta = \epsilon^2 dy^+ = \epsilon d\hat{y}$ and



(a)



(b)

FIG. 3: Reynolds stress peak value dependence on Reynolds number. (a). $1 - T_m^+$ versus Re_τ . (b). $(1 - T_m^+) / \sqrt{Re_\tau}$ versus Re_τ .

$dT^+ = \epsilon d\hat{T}$, there is a transparent matching between the meso equation 6 and the outer equation 2 as \hat{y} extends to the outer layer. The meso scaling should therefore be appropriate for the Reynolds stress data into the outer region as well.

The meso scaling of the Reynolds shear stress profiles is shown in FIG. 4. By the definition of \hat{T} and \hat{y} , all the profiles will lie to the point $(\hat{y} = 0, \hat{T} = 0)$. Note that \hat{T} is defined through the deficit of the Reynolds shear stress from its maximum value, therefore $\hat{T} \leq 0$. Using the estimation of $y_m^+ = O(\frac{1}{\epsilon})$, the extent of \hat{y} in FIG. 4 is

$$-O(1) < \hat{y} < O(\frac{1}{\epsilon}) \quad (7)$$

The meso scaling itself is theoretically valid at least for the region around $\hat{y} = 0$ with extent of $\Delta\hat{y} = O(1)$. As mentioned above, there is a transparent matching between meso scaling and outer scaling. Therefore the meso scaling extends throughout the

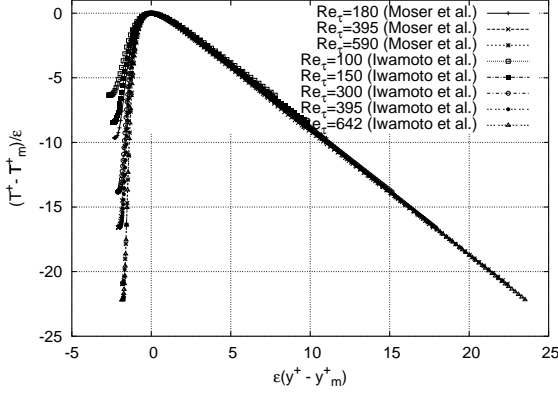


FIG. 4: Meso scaling of the Reynolds shear stress for different Reynolds number flows. Data are from the DNS of turbulent channel flows. Experimental data are not included, because of the difficulty in extracting precise y_m^+ and T_m^+ .

outer layer. This is strongly supported by the data shown in FIG. 4.

Formally applying the meso scaling, \hat{T} vs. \hat{y} (Eq. 5) to Reynolds shear stress requires knowledge of the peak Reynolds stress value and location, T_m^+ and y_m^+ , which are not necessarily known beforehand, and often difficult to precisely determine from data. However, the multiscale analysis of the mean momentum equation yields estimates for T_m^+ and y_m^+ , in agreement with the data of FIG.2 and FIG. 3.

Namely, as described in the previous section and derived in Wei et al., for sufficiently high Reynolds number the Reynolds stress peak location and value are shown to satisfy

$$y_m^+ = O\left(\frac{1}{\epsilon}\right), \quad T_m^+ = 1 - O(\epsilon). \quad (8)$$

Using these relations in the definition of \hat{T} and \hat{y} yields

$$\hat{T} = \frac{1}{\epsilon}(T^+ - 1) + O(1), \quad (9)$$

and

$$\hat{y} = \epsilon y^+ - O(1). \quad (10)$$

Therefore a plot of $\frac{1}{\epsilon}(T^+ - 1)$ versus ϵy^+ provides an alternate scaling to the “exact” meso scaling, \hat{T} versus \hat{y} , without the a priori knowledge of the peak location and magnitude of the Reynolds shear stress. This scaling is shown in FIG. 5(a) and 5(b). FIG. 5(a) is plotted on linear axes, emphasizing the outer region. FIG. 5(b) is plotted on semi-log axes, emphasizing the near wall region. Two features of this

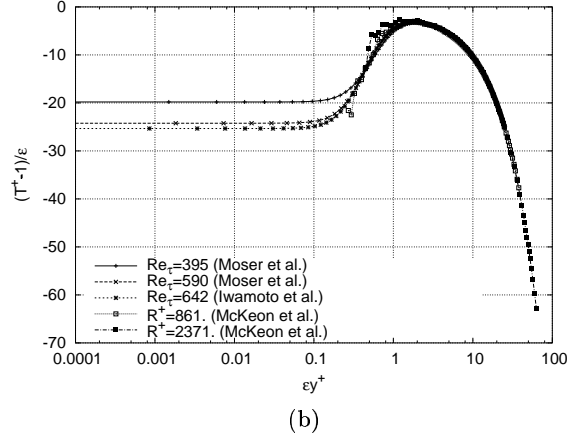
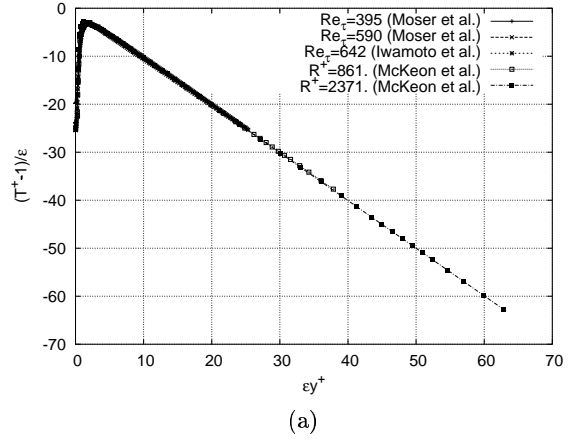


FIG. 5: Alternate meso scaling of Reynolds shear stress. (a). On linear scale. (b). Semi-log scale.

figure are reiterated: 1) The alternate meso scaling merges the maximum Reynolds stress locations and values to a single curve (should be within $O(1)$). This simply reflects that the correct scaling has been applied for the peak Reynolds stress ($T_m^+ = 1 - O(\epsilon)$) and its location ($y_m^+ = O(\frac{1}{\epsilon})$) in the definition of \hat{T} and \hat{y} . 2) The Reynolds stress profiles of different Reynolds numbers merge in the outer region under the approximate meso scaling. This is because of the reasons mentioned above.

V. CONCLUSIONS

In this paper the meso scaling of Wei et al.⁴ has been applied to the scaling of the Reynolds shear stress in turbulent channel and pipe flows. This scaling is shown to accurately characterize the Reynolds shear stress around the peak location of the Reynolds stress. Furthermore, the data convincingly support the meso scaling in the outer layer as

predicted by the theory of Wei et al.⁴. As a result the meso scaling is appropriate for Reynolds shear stress over a spatial domain extending from the lower boundary of the meso layer to the centerline.

Acknowledgments

This work was supported by the U. S. Department of Energy through the *Center for the Sim-*

ulation of Accidental Fires and Explosions under grant W-7405-ENG-48, the National Science Foundation under grant CTS-0120061 (grant monitor, M. Plesniak), and the Office of Naval Research under grant N00014-00-1-0753 (grant monitor, R. Joslin). Thanks are extended to Drs. Moser, Kasagi, McKeon and Wei for putting their data on the web for public use.

-
- ¹ D. DeGraaff and J. Eaton, *Reynolds-number scaling of the flat plate turbulent boundary layer*, J. Fluid Mech. **422**, 319 (2000).
- ² M. Gad-el-Hak and P. Bandyopadhyay, *Reynolds number effects in wall-bounded turbulent flows*, Applied Mechanics Reviews **47**, 307 (1994).
- ³ H. Tennekes and J. L. Lumley, *A First Course in Turbulence* (The MIT Press, Cambridge, Massachusetts, 1972).
- ⁴ T. Wei, P. Fife, J. Klewicki, and P. McMurtry, *Properties of the mean momentum balance in turbulent boundary layer, pipe and channel flows*, under review for J. Fluid Mech. (2004).
- ⁵ P. Fife, T. Wei, J. Klewicki, and P. McMurtry, *Stress gradient balance layers and scale hierarchies in wall-bounded turbulent flows*, under review for J. Fluid Mech. (2004).
- ⁶ P. Fife, J. Klewicki, P. McMurtry, and T. Wei, *Multiscale scaling in the presence of indeterminacy: wall-induced turbulence*, Under review for SIAM J. Multiscale Modeling and Simulation (2004).
- ⁷ R. R. Long and T.-C. Chen, *Experimental evidence for the existence of the mesolayer in turbulent systems*, J. Fluid Mech. **105**, 19 (1981).
- ⁸ K. R. Sreenivasan, in *Frontiers in Experimental Fluid Mechanics*, edited by Gad-el-Hak (Springer, New York, 1989), pp. 159–209.
- ⁹ N. Afzal, *Fully developed turbulent flow in a pipe: an intermediate layer*, Ingenieur-Archiv **52**, 355 (1982).
- ¹⁰ N. Afzal, *Mesolayer theory for turbulent flows*, AIAA J. **22**, 437 (1984).
- ¹¹ R. D. Moser, J. Kim, and N. N. Mansour, *Direct numerical simulation of turbulent channel flow up to $Re_\tau = 590$* , Physics of Fluids **11**, 943 (1999).
- ¹² K. Iwamoto, Y. Suzuki, and N. Kasagi, *Reynolds number effect on wall turbulence: Toward effective feedback control*, Int. J. Heat and Fluid Flow **23**, 678 (2002).
- ¹³ T. Wei and W. Willmarth, *Reynolds-number effects on the structure of a turbulent channel flow*, J. Fluid Mech. **204**, 57 (1989).
- ¹⁴ B. J. McKeon, J. Li, W. Jiang, J. F. Morrison, and A. J. Smits, *Pitot probe corrections in fully developed turbulent pipe flow*, Measurement Science and Technology **14**, 1449 (2003).